Time Refraction and Time Reflection above Critical Angle for Total Internal Reflection

Lior Bar-Hillel,[1] Alex Dikopoltsev,[2,3] Amit Kam,[2] Yonatan Sharabi,[2] Ohad Segal,[1] Eran Lustig,[2] and Mordechai Segev[1,2,*]

[1]*Department of Electrical and Computer Engineering, Technion, Haifa 32000, Israel*
[2]*Physics Department, Technion, Haifa 32000, Israel*
[3]*Institute of Quantum Electronics, ETH Zurich, 8093 Zurich, Switzerland*

(Received 24 October 2023; accepted 3 May 2024; published 27 June 2024)

We study the time reflection and time refraction of waves caused by a spatial interface with a medium undergoing a sudden temporal change in permittivity. We show that monochromatic waves are transformed into a pulse by the permittivity change, and that time reflection is enhanced at the vicinity of the critical angle for total internal reflection. In this regime, we find that the evanescent field is transformed into a propagating pulse by the sudden change in permittivity. These effects display enhancement of the time reflection and high sensitivity near the critical angle, paving the way to experiments on time reflection and photonic time crystals at optical frequencies.

DOI: 10.1103/PhysRevLett.132.263802

Modulating the electromagnetic (EM) properties of a medium at ultrafast timescales [1] is now gaining renewed interest due to recent advances in ultrafast switching in highly nonlinear materials [2–9]. Importantly, inducing an abrupt temporal change in the EM properties of a medium is fundamentally different from an abrupt change in space (an interface) because causality plays a crucial role. In the context of light-matter interactions, strong and abrupt changes in the refractive index result in time reflection and time refraction [1,10,11], and can yield a variety of phenomena ranging from fast switching of ultrastrong coupling [12–14] and localization by temporal disorder [15,16] to enhanced emission by dipoles [17], quantum fluctuations [17] and free electrons [18] in photonic time-crystals (PTCs), and time-varying dielectric media [19–25]. PTCs, photonic structures whose EM properties are varied periodically in time with a period comparable to a single cycle of a wave propagating therein, are perhaps the most promising manifestation of such strong abrupt variations in the refractive index [15,17,18,22,26–31]. As we show below, a wave incident upon a spatial interface with a time-varying medium exhibits unique properties.

When an EM wave propagates in a medium whose refractive index varies within a few cycles, the wave experiences refractions and reflections known as "time refractions" and "time reflections" [10,11]. When the medium is homogeneous, both time refraction and time reflection are manifested in the translation of the temporal spectrum, as a consequence of momentum conservation. The time-refracted wave continues to propagate with the same wave vector, whereas the time-reflected wave is propagating backwards with a conjugate phase (due to the sign change in the frequency) [7,11,32]. Importantly, while time refraction is always significant, for the time reflection to be measurable, the index change has to be large (order of unity) and abrupt (occurring within 1–2 optical cycles), otherwise the time reflection is extremely weak, and PTCs become unfeasible. This tough requirement to have a strong and abrupt change in the refractive index is the reason why time reflection of light has never been observed at optical frequencies. Thus far time reflection was observed with water waves [32] and cold atoms [33] and was proposed in synthetic dimensions [34], but with EM waves, it was observed only at microwave frequencies [35,36]. The reason it is extremely hard to observe time reflections at optical frequencies is profound: many nonlinear optics effects are instantaneous (e.g., the optical Kerr effect), but the index change they yield is at least 1000-fold too weak to cause measurable time reflections. At the other extreme, some nonlinear effects can provide huge index changes, but their response is orders of magnitude too slow to drive time reflections because they require transport (of charges, of atoms, etc.). There are only a handful of exceptions: mechanisms giving rise to large index changes occurring within a few femtoseconds (fsec). One of those involves transparent conductive oxides, where recent work has demonstrated index changes of ~ 0.3 within 5–8 fsec [8,9,37]. Those experiments showed that there is indeed a mechanism that makes time reflections and PTCs feasible at optical frequencies. However, even in that experiment—time reflection was too weak to be measured. These recent experimental results imply that new approaches are needed to achieve substantial time reflection at optical frequencies.

Here, we study time reflection and time refraction of waves incident upon an interface with a dielectric medium experiencing a sudden temporal change. We show that a monochromatic wave incident upon such an interface

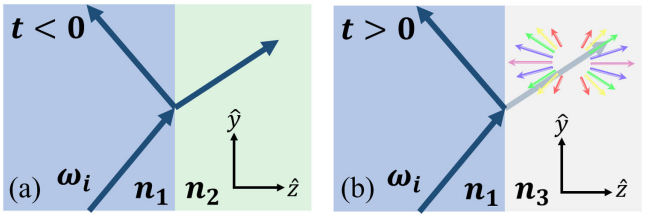

FIG. 1. (a) A monochromatic plane-wave incident upon a spatial interface undergoes refraction and reflection while conserving its original frequency ω_i. (b) A monochromatic plane wave incident upon a spatial interface with a medium that at $t = 0$ undergoes an abrupt change in its refractive index from n_2 to n_3. The abrupt index change gives rise to the appearance of a continuous spectrum of waves, where each frequency propagates at a different angle such that higher frequencies are concentrated along the z horizonal axis. Thus, both the time-refracted and the time-reflected waves form spatiotemporal wave packets which spread during their propagation.

transforms into pulses. We find that the time reflection is enhanced near total internal reflection (TIR), especially at the critical angle which acts as an exceptional point [38–42]. For incidence above the critical angle, we find that the evanescent wave penetrating into the time-varying medium is transformed into time-refracted and time-reflected propagating (nonevanescent) pulses. The process described here can be applied to analyze various photonic systems involving spatial interfaces with suddenly changing dielectric media, and can enable the first experimental demonstration of a PTC at optical frequencies.

Let us begin with the standard case of a monochromatic plane wave at frequency ω propagating in a one-dimensional homogenous medium that at $t = 0$ experiences a sudden temporal change in its refractive index from n_1 to n_2. Maxwell's equations dictate boundary conditions at $t = 0$ such that the electric displacement and magnetic flux density vectors are continuous in time [10]. These conditions give rise to backward and forward propagating waves for $t > 0$. Since the medium is homogeneous, momentum is conserved, hence both of those waves have the same wave vector as the original wave, but at different frequencies $\omega'_{\pm} = \pm\omega(n_1/n_2)$. The forward wave is the time refraction and has positive frequency, whereas the backward wave is the time reflection, which has "negative" frequency. The physical consequences of the negative frequency are that the time-reflected wave propagates backwards in space with a conjugate phase. For simplicity, we assume that the electric displacement reacts instantaneously to the change in the electric field. Under this assumption, the refraction and reflection coefficients (for amplitudes) for an instantaneous index change (a temporal interface) are $t_{\text{time}} = \frac{1}{2}((n_1/n_2)^2 + (n_1/n_1))$ and $r_{\text{time}} = \frac{1}{2}((n_1/n_2)^2 - (n_1/n_2))$ [10,43,44]. Thus, to obtain significant time reflection, the change in refractive index has to be large.

Next, we explore the nature of those phenomena for a monochromatic plane-wave incident upon a spatial interface with a time-varying medium. To do that properly, consider first the simple example of a spatial interface between two media. The interface is in the xy plane, where for $z < 0$ the refractive index is n_1 and for $z > 0$ the index is $n_2 < n_1$. At time $t = 0$ the second medium experiences a sudden temporal change such that its refractive index changes to n_3. We denote $\theta_{c,1}$ and $\theta_{c,2}$ as the critical angles for TIR before and after the temporal change, respectively. In this setting, a plane wave of frequency ω_i, wave vector $\vec{k}_i = (0, k_y, k_z)$ and amplitude $E_i = 1$ is incident upon this interface at angle θ_i, as sketched in Fig. 1. To calculate the evolution of the EM fields for $t > 0$, we carry out the following process. Using the known fields at $t = 0^-$ and the temporal boundary conditions, we find the EM fields at $t = 0^+$, project the fields onto the eigenmodes of the system after the sudden change, evolve each eigenmode in time separately, and reconstruct the total EM fields using superposition. This process holds for every wave system that varies abruptly in time. We apply this process on the example described above for a TE polarized plane wave, and for simplicity set $n_3 = n_1$. We focus on the region $z > 0$. After the sudden temporal change, the waves are characterized by their wave vectors and the dispersion $\omega(\vec{k}) = \pm(c/n_1)|\vec{k}|$. By projecting the fields on the eigenmode basis, we find the amplitudes of the time-reflected waves $E^-(\vec{\kappa})$, which correspond to the negative branch of the dispersion curve, and the amplitudes of the time-refracted waves $E^+(\vec{\kappa})$ which correspond to the positive branch, as described by

$$E^{\pm}(\kappa_z, \kappa_y) = \frac{t_F}{2}\left(\left(\frac{n_2}{n_1}\right)^2 \pm \frac{\omega(\vec{\kappa})}{\omega_i}\frac{\kappa_y k_y + \kappa_z \beta}{\kappa_y^2 + \kappa_z^2}\right) \times \left(\frac{1}{i(\beta - \kappa_z)} + \pi\delta(\kappa_z - \beta)\right)\delta(\kappa_y - k_y). \quad (1)$$

We denote t_F as the Fresnel transmission coefficient and $\beta = (\omega_i/c)\sqrt{n_2^2 - n_1^2 \sin^2\theta_i}$ as the propagation constant of the original wave in the z direction. The critical angle for TIR occurs when the square root is zero, above it β is imaginary. The amplitudes of the time-reflected waves are shown in Fig. 2(a) for $n_1 = n_3 = 0.8$ and $n_2 = 0.3$. An index change of this magnitude is feasible, as demonstrated recently in epsilon near zero martials [9]. The symmetric curves shown in Fig. 2(a) are explained as follows: for $t < 0$, above $\theta_{c,1}$ the EM field in the region $z > 0$ is an evanescent wave, and as such it is spatially localized very close to the interface. The strong variation in the refractive index at $t = 0$ causes time reflection, but the wave has no spatial preference, hence the time-reflected waves evolve in the same manner towards both sides of the interface. We see that Eq. (1) displays high sensitivity in the vicinity of $\theta_{c,1}$, due to the transition from a purely real to a purely imaginary value of β. Prior to the abrupt change in refractive index, the imaginary propagation constant leads

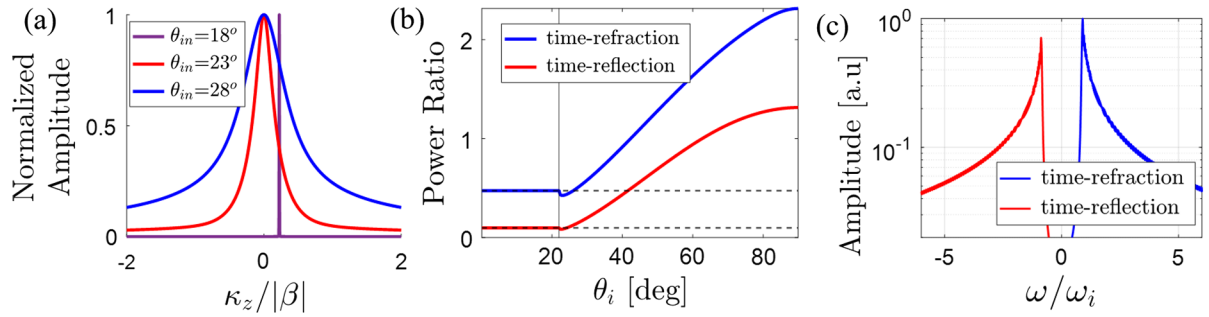

FIG. 2. Analytic results of the time refraction and time reflection induced by a sudden change of a dielectric interface for $\boldsymbol{n}_3 = \boldsymbol{n}_1 = 0.8$ and $\boldsymbol{n}_2 = 0.3$. The critical angle for TIR is $\theta_{c,1} = 22°$. (a) Normalized amplitudes of the time-reflected waves vs normalized propagation constant in the z direction, for 3 different incidence angles. Below θ_C (blue) the Fresnel-refracted wave has a real propagation constant, hence so does the time-reflected wave, and the spectrum is a delta function commensurate with Snell's law. Above $\theta_{c,1}$ the propagation constant of the time-reflected wave is complex, always localized at normal incidence, and has a broader spectrum as the angle is increased above TIR. (b) Ratio between the time-reflected and time-refracted powers to the incident power (defined as the power in the region $z > 0$ at $t < 0$), as a function of the angle of incidence. $\theta_{c,1}$ is marked by a vertical black line. (c) Spectrum of the time refraction and time reflection for angle of incident $\theta_i = 50°$.

to a complex polarization of the magnetic field, resulting in a relative phase of $(\pi/2)$ between the transverse components of the electric and magnetic fields. As a consequence, the time-average Poynting vector in the z direction, indicative of the photon flux, is zero. However, following the sudden change, a mismatch between the new impedance of the medium and the wave impedance (the ratio between the electric and magnetic fields) is created, altering the relative phase between the fields and leading to a nonzero photon flux in the z direction. Time reflection is then induced to reconcile this phase difference and impedance mismatch. The enhancement of the time reflection near the critical angle for TIR and the sensitivity are similar to other enhancement effects observed at the vicinity of that angle [45,46], because that angle is an exceptional point.

Notice that each time-reflected and time-refracted plane wave has a different frequency according to the dispersion curve, and propagates at a different angle, as sketched in Fig. 1(b). The relation between the propagation angle and the frequency can be extracted from momentum conservation in the y direction, which Eq. (1) manifests for the special case $n_3 = n_1$ as the delta function dictates the same k_y for all waves, and is given by

$$\omega(\theta)\sin\theta n_3 = \omega_i \sin\theta_i n_1. \tag{2}$$

We see from Eq. (2) that, for a given input wave at ω_i and θ_i, the larger the ratio (n_1/n_3) the larger the frequency shift $\omega(\theta) - \omega_i$, and the more the time-refracted and time-reflected spatio-temporal wave packets spread in space as the relative angles of propagation between waves with adjacent frequencies increase. Notably, above $\theta_{c,1}$, the higher the angle of incidence, the broader the spectrum of plane waves [Fig. 2(a)]. Waves with higher κ_z have higher frequencies, thus the spectrum of the time reflection and time refraction is broader. For higher values of (n_2/n_1), β increases, resulting in a wider bandwidth.

The abrupt index change transforms the evanescent wave into a propagating wave, for both the time-refracted and the time-reflected waves. We use Parseval's theorem to estimate the power of the time-reflected and time-refracted waves, displayed in Fig. 2(b). The power fraction that is time reflected is highly enhanced above the critical angle, exceeding 100% of the power of the original wave. For waves incident below $\theta_{c,1}$, the time-reflected power fraction is the same as the reflected power for a plane wave propagating in a homogenous medium whose refractive index is changed abruptly from 0.3 to 0.8 [lower dashed black line in Fig. 2(b)], approximately 9.8% of the power of the original wave. Hence, below the critical angle, the time-reflected power from the interface with a medium undergoing a step change in its refractive index coincides with the simple case of time reflection of a plane wave in a homogeneous medium, with the reflection coefficient given above. This means that the time-reflected power is enhanced above the critical angle, enhancement that can even reach an order of magnitude compared to the time reflection below the critical angle.

Up to this point, we provided analytical analysis of the case in which the optical properties of the system undergo an abrupt change, after which the entire space is homogeneous. We proceed with a numerical study on the time reflection of a pulse incident on the same dielectric interface, by numerically solving Maxwell's equations for different scenarios. For the simulation, we employ the 2D finite difference Time-domain (FDTD) method. We create a simulation area, with a dielectric interface at $z = 0$ between $n_1 = 1.5$ at $z < 0$ and $n_2 = 0.3$ for $z > 0$. We launch a TE-polarized pulsed Gaussian beam with a mean frequency $\omega_i = 2 \times 10^{15}$ (rad/s) toward the interface, as illustrated [Fig. 3(a)]. At time $t = 0$, when the peak of the

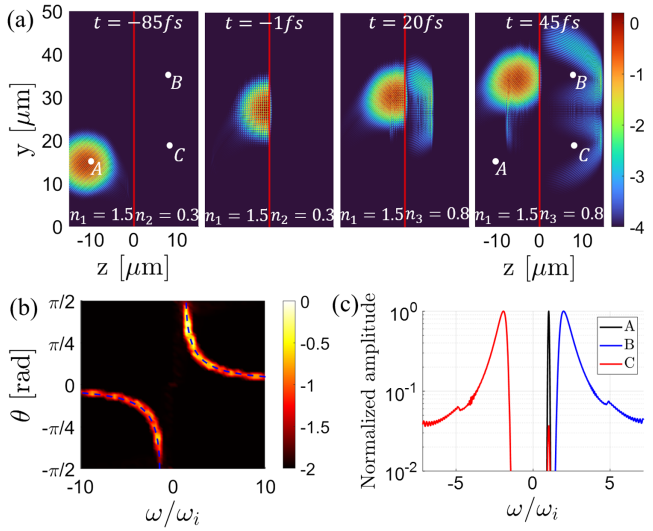

FIG. 3. Simulations showing the time-refraction and time-reflection of a pulse, induced by a sudden change of a dielectric interface for $\boldsymbol{n}_1 = 1.5$, $\boldsymbol{n}_2 = 0.3$, and $\boldsymbol{n}_3 = 0.8$. (a) A pulsed Gaussian beam is launched toward a dielectric interface positioned at $z = 0$ (vertical red line). The EM fields at points A, B, and C are being sampled as the simulation evolves in time. The pulse is incident at incidence angle of $\theta_i = 50°$, which is above $\theta_{c,1}$, hence at $t < 0$ the photon flux in the z direction is zero for $z > 0$. At $t = 0$ the refractive index in the region $z > 0$ is changed to $n_3 = 0.8$, so the angle of incident remains above the new critical angle, $\theta_{c,2}$. (b) Normalized amplitudes (log scale) of the waves that make up the electric field in the region $z > 0$ at time $t = 45$ fs vs their frequency and angle of propagation. The theoretical curve according to Eq. (2) is marked by the blue dashed line. (c) Normalized spectrum of the incident pulse (black) sampled at the point A in (a), along with the spectra of the time-refracted (blue) and time-reflected (red) pulses sampled at the points B and C in (a). The color bar in (a) represents light intensity (log scale), normalized to the peak intensity of the original pulse.

pulse reaches the interface, we change the refractive index in the region $z > 0$ to $n_3 = 0.8$, such that the critical angle becomes smaller, $\theta_{c,2} < \theta_{c,1} < \theta_i$. We choose the indices of refraction according to recent experiment [9] in which time refraction was observed in the regime of a single optical cycle. To obtain meaningful information we choose points in space (A, B, C) through which the incident, the time-reflected and the time-refracted pulses, pass and sample the pulses in time. Using these time samples, we determine the spectrum of each pulse. The simulation results, along with the spectra of the incident pulse, time reflection and time refraction, are presented in Figs. 3(a) and 3(c), respectively.

By examining the result of the simulation, we find 5 pulses after the sudden change in the reflective index, as shown in Fig. 3(a). The original pulse is reflected by the temporal change because after the sudden change it stays above the critical angle of TIR. There are two time-refracted pulses which have positive propagation constant in the y direction. One of the time-refracted pulses overlaps with the Fresnel reflection of the original pulse from the spatial interface, while the other passes through point C. Lastly, we see two time-reflected pulses, one of them passes through point B, while the other propagates toward point A. Before the abrupt change we find zero photon flux in the z direction in the region $z > 0$. After the abrupt temporal change we find that the index variation gives rise to nonzero photon flux in the z direction, carried by both the time-reflected and time-refracted pulses. We see that the time reflection and time refraction are constructed of waves of different frequencies, each propagates in a different direction, Fig. 3(a) at time $t = 45$ fs. Figure 3(b) shows the wave amplitudes as a function of their propagation angle and frequency along with our theoretical curve following Eq. (2). To analyze the fields recorded at points A, B, and C we calculate their spectra, Fig. 3(c). The spectra of the time-reflected and time-refracted pulses have similar shapes, differing due to slight asymmetry between points B, C, and the center of the pulse, and are broadbanded with respect to the initial pulse. A simple estimation reveals that this broadening of the bandwidth cannot solely be attributed to the bandwidth of the initial pulse. As a sanity check, in a spatially-homogeneous time-boundary, the new bandwidth would be narrower by a factor of $(n_2/n_3) \approx 0.4$, significantly smaller than the observed broadening in Fig. 3(c). Thus, this broadening is affected strongly by the spatial interface. To further support our theoretical analysis, we simulate a case of a cw laser beam which is closer in nature to a plane wave. The results are presented in Sec. B of [44].

Finally, to complement the study, we simulate several chosen cases of the time-varying interface. The scenarios, described in Sec. A of [44] and the figures therein, are similar to that of Fig. 3, with the abruptly varied refractive indices causing a change in the critical angle of TIR from $\theta_{c,1}$ to $\theta_{c,2}$. In addition to the case presented in Fig. 3 where $\theta_{c,2} < \theta_{c,1} < \theta_i$, we examine three additional generic cases. (i) $\theta_{c,1} < \theta_i < \theta_{c,2}$, (ii) $\theta_{c,1} < \theta_{c,2} < \theta_i$, and (iii) $\theta_{c,2} < \theta_i < \theta_{c,1}$, Fig. 4. We observe that the abrupt change in the refractive index transforms the incident monochromatic wave propagating (nonevanescent) time-reflected and time-refracted pulses, each carrying energy in the z direction. Generally, we notice that for incidence above the critical angle with a larger ratio n_2/n_1, the spectra of the time-reflection and time-refraction pulses are broader, and the higher the ratio n_1/n_3 the higher their central frequencies are, as expected from the analysis following Eq. (2). In addition, we examine cases of slower variations of the refractive index, reaching a rate of the single cycle of the EM pulse, Sec. C in [44]. We find that the time reflection is strongly affected by the variation time of the refractive index, being much stronger for abrupt changes. Nevertheless, the main features of the time refraction and time reflection described here are all observable for noninstantaneous yet fast enough variation of the refractive index.

To conclude, we studied the reflection and refraction of EM waves from a dielectric interface with a medium undergoing an abrupt change in the refractive index, and focused on the effects near TIR. We found that monochromatic waves are transformed into time-refracted and time-reflected multispectral waves that form pulses. Beyond the critical angle for TIR, the evanescent waves are transformed into propagating pulses and the time reflection is enhanced. The concepts discussed here can be extended to reflection and refraction by a spatiotemporal interface [47,48], and are expected to display similar results. Our findings raise several intriguing questions. For example, is it possible to design an optical structure that enhances time reflection and reduces time refraction? Do spatial evanescent modes exist in a PTC? How does TIR affect the Floquet modes at an interface of PTC and a dielectric medium? Finally, this work helps design the experimental scheme for the observation of time reflection at optical frequencies.

This research was supported by a Grant No. 2032635: FA8655-22-1-7256 from the Air Force Office of Scientific Research, and by the Breakthrough Program of the Israel Science Foundation.

*Corresponding author: msegev@technion.ac.il

[1] F. R. Morgenthaler, Velocity modulation of electromagnetic waves, IRE Trans. Microwave Theory Tech. **6**, 167 (1958).
[2] N. Kinsey, C. DeVault, J. Kim, M. Ferrera, V. M. Shalaev, and A. Boltasseva, Epsilon-near-zero Al-doped ZnO for ultrafast switching at telecom wavelengths, Optica **2**, 616 (2015).
[3] L. Caspani *et al.*, Enhanced nonlinear refractive index in ε-near-zero materials, Phys. Rev. Lett. **116**, 233901 (2016).
[4] M. Z. Alam, I. De Leon, and R. W. Boyd, Large optical nonlinearity of indium tin oxide in its epsilon-near-zero region, Science **352**, 795 (2016).
[5] Y. Zhou, M. Z. Alam, M. Karimi, J. Upham, O. Reshef, C. Liu, A. E. Willner, and R. W. Boyd, Broadband frequency translation through time refraction in an epsilon-near-zero material, Nat. Commun. **11**, 1 (2020).
[6] O. Reshef, I. De Leon, M. Z. Alam, and R. W. Boyd, Nonlinear optical effects in epsilon-near-zero media, Nat. Rev. Mater. **4**, 8 (2019).
[7] V. Bruno, S. Vezzoli, C. DeVault, E. Carnemolla, M. Ferrera, A. Boltasseva, V. M. Shalaev, D. Faccio, and M. Clerici, Broad frequency shift of parametric processes in epsilon-near-zero time-varying media, Appl. Sci. **10**, 4 (2020).
[8] E. Lustig, S. Saha, E. Bordo, C. DeVault, S. N. Chowdhury, Y. Sharabi, A. Boltasseva, O. Cohen, V. M. Shalaev, and M. Segev, Towards photonic time-crystals: Observation of a femtosecond time-boundary in the refractive index, in *Proceedings of the 2021 Conference on Lasers and Electro-Optics (Cleo)* (2021), pp. 1–2.
[9] E. Lustig *et al.*, Time-refraction optics with single cycle modulation, Nanophotonics **12**, 2221 (2023).
[10] J. T. Mendonça and P. K. Shukla, Time refraction and time reflection: Two basic concepts, Phys. Scr. **65**, 160 (2002).
[11] F. Biancalana, A. Amann, A. V. Uskov, and E. P. O'Reilly, Dynamics of light propagation in spatiotemporal dielectric structures, Phys. Rev. E **75**, 046607 (2007).
[12] G. Günter *et al.*, Sub-cycle switch-on of ultrastrong light–matter interaction, Nature (London) **458**, 7235 (2009).
[13] C. M. Wilson, G. Johansson, A. Pourkabirian, M. Simoen, J. R. Johansson, T. Duty, F. Nori, and P. Delsing, Observation of the dynamical casimir effect in a superconducting circuit, Nature (London) **479**, 7373 (2011).
[14] M. Halbhuber, J. Mornhinweg, V. Zeller, C. Ciuti, D. Bougeard, R. Huber, and C. Lange, Non-adiabatic stripping of a cavity field from electrons in the deep-strong coupling regime, Nat. Photonics **14**, 11 (2020).
[15] Y. Sharabi, E. Lustig, and M. Segev, Disordered photonic time crystals, Phys. Rev. Lett. **126**, 163902 (2021).
[16] B. Apffel, S. Wildeman, A. Eddi, and E. Fort, Experimental Implementation of wave propagation in disordered time-varying media, Phys. Rev. Lett. **128**, 094503 (2022).
[17] M. Lyubarov, Y. Lumer, A. Dikopoltsev, E. Lustig, Y. Sharabi, and M. Segev, Amplified emission and lasing in photonic time crystals, Science **377**, 425 (2022).
[18] A. Dikopoltsev, Y. Sharabi, M. Lyubarov, Y. Lumer, S. Tsesses, E. Lustig, I. Kaminer, and M. Segev, Light emission by free electrons in photonic time-crystals, Proc. Natl. Acad. Sci. U.S.A. **119**, e2119705119 (2022).
[19] J. R. Zurita-Sánchez, P. Halevi, and J. C. Cervantes-González, Reflection and transmission of a wave incident on a slab with a time-periodic dielectric function $\epsilon(t)$, Phys. Rev. A **79**, 053821 (2009).
[20] J. R. Zurita-Sánchez, J. H. Abundis-Patiño, and P. Halevi, Pulse propagation through a slab with time-periodic dielectric function $\varepsilon(t)$, Opt. Express **20**, 5586 (2012).
[21] J. R. Reyes-Ayona and P. Halevi, Observation of genuine wave vector (k or β) gap in a dynamic transmission line and temporal photonic crystals, Appl. Phys. Lett. **107**, 074101 (2015).
[22] E. Lustig, Y. Sharabi, and M. Segev, Topological aspects of photonic time crystals, Optica **5**, 1390 (2018).
[23] J. Sloan, N. Rivera, J. D. Joannopoulos, and M. Soljačić, Controlling two-photon emission from superluminal and accelerating index perturbations, Nat. Phys. **18**, 1 (2022).
[24] E. Galiffi, R. Tirole, S. Yin, H. Li, S. Vezzoli, P. A. Huidobro, M. G. Silveirinha, R. Sapienza, A. Alù, and J. B. Pendry, Photonics of time-varying media, Adv. Opt. Photonics **4**, 014002 (2022).
[25] S. A. R. Horsley and J. B. Pendry, Quantum electrodynamics of time-varying gratings, Proc. Natl. Acad. Sci. U.S.A. **120**, e2302652120 (2023).
[26] V. Pacheco-Peña and N. Engheta, Temporal aiming, Light Sci. Appl. **9**, 1 (2020).
[27] V. Pacheco-Peña and N. Engheta, Temporal equivalent of the Brewster angle, Phys. Rev. B **104**, 214308 (2021).

[28] Y. Sharabi, A. Dikopoltsev, E. Lustig, Y. Lumer, and M. Segev, Spatiotemporal photonic crystals, Optica **9**, 585 (2022).
[29] E. Lustig, O. Segal, S. Saha, C. Fruhling, V. M. Shalaev, A. Boltasseva, and M. Segev, Photonic time-crystals—fundamental concepts, Opt. Express **31**, 9165 (2023).
[30] S. Saha, O. Segal, C. Fruhling, E. Lustig, M. Segev, A. Boltasseva, and V. M. Shalaev, Photonic time crystals: A materials perspective, Opt. Express **31**, 8267 (2023).
[31] X. Wang, M. S. Mirmoosa, V. S. Asadchy, C. Rockstuhl, S. Fan, and S. A. Tretyakov, Metasurface-based realization of photonic time crystals, Sci. Adv. **9**, eadg7541 (2023).
[32] V. Bacot, M. Labousse, A. Eddi, M. Fink, and E. Fort, Time reversal and holography with spacetime transformations, Nat. Phys. **12**, 972 (2016).
[33] Z. Dong, H. Li, T. Wan, Q. Liang, Z. Yang, and B. Yan, Quantum time reflection and refraction of ultracold atoms, Nat. Photonics **18**, 68 (2023).
[34] O. Y. Long, K. Wang, A. Dutt, and S. Fan, Time reflection and refraction in synthetic frequency dimension, Phys. Rev. Res. **5**, L012046 (2023).
[35] H. Moussa, G. Xu, S. Yin, E. Galiffi, Y. Ra'di, and A. Alù, Observation of temporal reflection and broadband frequency translation at photonic time interfaces, Nat. Phys. **19**, 6 (2023).
[36] T. R. Jones, A. V. Kildishev, and D. Peroulis, Time-Reflection of Microwaves by a Fast Optically-Controlled Time-Boundary, arXiv:2310.02377.
[37] R. Tirole, S. Vezzoli, E. Galiffi, I. Robertson, D. Maurice, B. Tilmann, S. A. Maier, J. B. Pendry, and R. Sapienza, Double-slit time diffraction at optical frequencies, Nat. Phys. **19**, 7 (2023).
[38] S. Klaiman, U. Günther, and N. Moiseyev, Visualization of branch points in PT-symmetric waveguides, Phys. Rev. Lett. **101**, 080402 (2008).
[39] O. Peleg, M. Segev, G. Bartal, D. N. Christodoulides, and N. Moiseyev, Nonlinear waves in subwavelength waveguide arrays: Evanescent bands and the "Phoenix Soliton", Phys. Rev. Lett. **102**, 163902 (2009).
[40] C. E. Rüter, K. G. Makris, R. El-Ganainy, D. N. Christodoulides, M. Segev, and D. Kip, Observation of parity–time symmetry in optics, Nat. Phys. **6**, 3 (2010).
[41] B. Alfassi, O. Peleg, N. Moiseyev, and M. Segev, Diverging Rabi oscillations in subwavelength photonic lattices, Phys. Rev. Lett. **106**, 073901 (2016).
[42] R. El-Ganainy, K. Makris, M. Khajavikhan *et al.*, Non-Hermitian physics and PT symmetry, Nature Phys. **14**, 11 (2018).
[43] L. Bar-Hillel, A. Dikopoltsev, Y. Sharabi, E. Lustig, A. Shmuel, and M. Segev, Time-reflection beyond the critical angle, *in Conference on Lasers and Electro-Optics (2022), Paper FTh5A.6* (Optica Publishing Group, 2022).
[44] See Supplemental Material at http://link.aps.org/supplemental/10.1103/PhysRevLett.132.263802 for additional numerical study of pulses incident on a time-varying dielectric boundary, and analytical derivation of our theoretical analysis.
[45] H. Herzig Sheinfux, I. Kaminer, Y. Plotnik, G. Bartal, and M. Segev, Subwavelength multilayer dielectrics: Ultrasensitive transmission and breakdown of effective-medium theory, Phys. Rev. Lett. **113**, 243901 (2014).
[46] H. H. Sheinfux, Y. Lumer, G. Ankonina, A. Z. Genack, G. Bartal, and M. Segev, Observation of Anderson localization in disordered nanophotonic structures, Science **356**, 953 (2017).
[47] S. A. R. Horsley and J. B. Pendry, Quantum electrodynamics of time-varying gratings, Proc. Natl. Acad. Sci. U.S.A. **120**, e2302652120 (2023).
[48] Z. Li, X. Ma, A. Bahrami, Z.-L. Deck-Léger, and C. Caloz, Generalized total internal reflection at dynamic interfaces, Phys. Rev. B **107**, 115129 (2023).